Resonances Produced in the Reaction $\pi^- p \to \pi^-\pi^-\pi^+ p$ at 8 GeV/c*

J. W. Lamsa, N. M. Cason, N. N. Biswas, I. Derado,† T. H. Groves, V. P. Kenney, J. A. Poirier, and W. D. Shephard

Department of Physics, University of Notre Dame, Notre Dame, Indiana

(Received 9 October 1967)

A study has been made of the reaction $\pi^- p \to \pi^-\pi^-\pi^+ p$ at an incident momentum of 8.05 GeV/c. We find this reaction to be very peripheral and dominated by production of the ρ^0 and the $N^{*++}(1236)$. The A_2 meson and an additional $\pi^-\rho^0$ enhancement at 1190 MeV are observed. The spins and parities of these resonances are examined with particular attention to the effect of the type and amount of background assumed. There has been much interest in higher-mass boson resonances; we here examine an enhancement in the 3π mass distribution at 1610 MeV which appears to decay primarily to $\pi^- f^0$. An enhancement in the $\pi^-\pi^+ p$ system near 1400 MeV is observed. We find that this enhancement cannot be explained by a Deck-type production mechanism, and conclude that the enhancement is due to production of the Roper resonance, the $N^*(1400)$.

I. INTRODUCTION

RECENT studies[1] of the reaction

$$\pi^- p \to \pi^-\pi^-\pi^+ p \tag{1}$$

have shown that this reaction is dominated by pseudo-three-body final states such as

$$\pi^- p \to \pi^-\rho^0 p\,, \tag{2}$$

$$\pi^- p \to \pi^-\pi^- N^{*++}(1236)\,, \tag{3}$$

and

$$\pi^- p \to \pi^- f^0 p\,. \tag{4}$$

These studies have concentrated on reaction (2) where resonances in the $\pi\rho$ system (the A mesons) have been observed and analyzed. The purpose of this study has been to examine reactions (2), (3), and (4) in order to determine what resonances and/or kinematic enhancements are present and to investigate their properties.

II. EXPERIMENTAL PROCEDURE

In this experiment approximately 50 000 photographs were obtained at Brookhaven National Laboratory (BNL) in the 80-in. hydrogen bubble chamber. The BNL dc-separated beam operating in the unseparated mode produced a π^- incident beam from the AGS at a momentum of 8.050 ± 0.040 GeV/c. The film was scanned for four-prong events in a fiducial region 1 m long with a minimum track length of 35 cm for secondary tracks going in the forward direction. The scan yielded 20 405 events having no visible strange particles definitely associated with them. These events were measured on both film-plane and image-plane measuring projectors.[2]

The analysis was carried out using the geometry and kinematics programs HGEOM[3] and GRIND.[4] Ambiguities with other hypotheses and ambiguities between π^+ and proton within reaction (1) were resolved by visually inspecting the bubble density of the tracks. We have retained four-constraint fits which remained ambiguous with other one-constraint hypotheses. A small sample of 21 events remained with π^+/proton track ambiguities within reaction (1). For these 21 events, the hypothesis with the lower χ^2 was chosen.

In order to insure a pure sample of reaction (1), the events were further required to have a χ^2 probability $>1\%$ and to have the square of their missing mass between ±0.02 GeV^2. The missing-mass-squared distribution is shown in Fig. 1. It has a central value of -0.0005 GeV^2 with a full width at half-maximum of 0.003 GeV^2. There is no evidence for contamination from events with an additional π^0. This selection procedure yielded 1973 $\pi^-\pi^-\pi^+ p$ events.

III. TWO-PARTICLE RESONANCES

Some of the basic features of reaction (1) are shown in the scatter diagram of $\pi^-\pi^+$ versus $\pi^+ p$ effective mass in Fig. 2. Strong ρ^0 and $N^{*++}(1236)$ bands are evident. An interesting feature of this scatter diagram

* Research supported in part by the National Science Foundation.

† Present address: Stanford Linear Accelerator Center, Stanford University, Stanford, Calif.

[1] V. E. Barnes, W. B. Fowler, K. W. Lai, S. Orenstein, D. Radojičić, M. S. Webster, A. H. Bachman, P. Baumel, and R. M. Lea, Phys. Rev. Letters **16**, 41 (1966); N. M. Cason, Phys. Rev. **148**, 1282 (1966); J. F. Allard, J. Hennessy, R. Huson, A. Lloret, J. Six, J. J. Veillet, G. Bellini, M. di Corato, E. Fiorini, P. Negri, and M. Rollier, Nuovo Cimento **50A**, 106 (1967).

[2] Both film-plane and image-plane measuring projectors proved quite satisfactory for measurement of interactions at 8 GeV/c. The film-plane projector provided somewhat better measurement precision but the image-plane projectors allowed a significantly higher measurement rate. Factors independent of the measuring projector, including operator setting error, uncertainties in chamber optics, and effects, such as turbulence in the chamber, seemed to dominate in the reconstruction of tracks. Thus, although the inherent precision of the film-plane machine was 2–3.5 times better than that for the image-plane machines, mean values of the rms deviation of measured points from the fitted track were larger for the image-plane projectors by factors of only 1.5–2. The kinematic fitting program further decreases the effects of differences among the machines. After kinematic fitting, mass resolutions for the different machines differed by factors of no more than 1.3–1.5. As an example, for $\pi^-\pi^-\pi^+$ effective masses between 1.1 and 1.4 GeV, the mass resolutions were 6.5, 8.8, and 9.1 MeV, respectively, for the one film-plane and two image-plane machines.

[3] J. W. Burren and J. Sparrow, Rutherford High Energy Laboratory Report No. NIRL/R/14, 1963 (unpublished). The program has been somewhat modified at Argonne National Laboratory and at the University of Notre Dame.

[4] R. Böck, CERN Internal Report No. DD/EXP/62/10, 1962 (unpublished); CERN TC Program Library (unpublished).

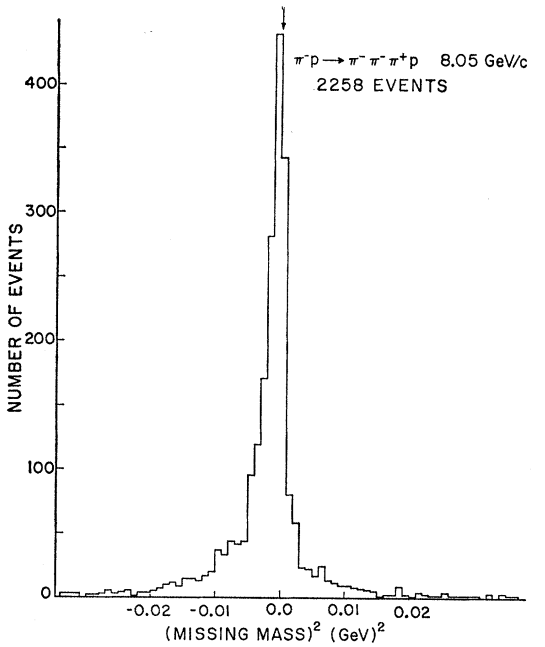

FIG. 1. Distribution of missing mass squared for the reaction $\pi^-p \to \pi^-\pi^-\pi^+p$. The arrow is located at 0.0 GeV^2.

is the high density of events at low $M(\pi^-\pi^+)$ in the N^{*++} band. This feature, which has been noted in other experiments,[5] may be caused by the strong low-mass enhancement in the π^-N^{*++} effective-mass distribution (see Sec. VI). This π^-N^{*++} peak at 1400 MeV has a Q value of only about 180 MeV, so that every event in the peak must have a low $\pi^-\pi^+$ mass.

The $\pi^-\pi^+$ and π^+p effective-mass projections are shown in Figs. 3 and 4. In addition to the strong ρ^0 peak in Fig. 3, a small f^0 enhancement is present. The π^+p mass distribution shows a strong $N^{*++}(1236)$ with no evidence for production of higher mass isobars.

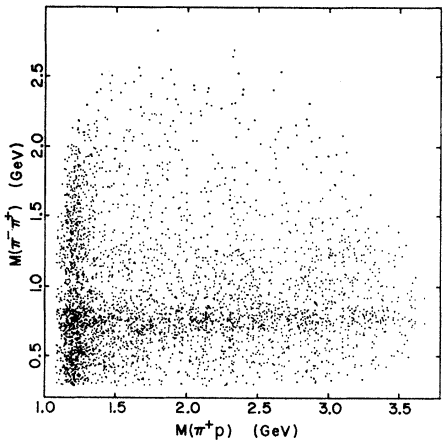

FIG. 2. Scatter diagram of $M(\pi^-\pi^+)$ versus $M(\pi^+p)$. Two points are plotted for each of the 1973 events.

[5] J. M. Shpiz, K. W. Lai, and M. S. Webster, Phys. Rev. **153**, 1722 (1967).

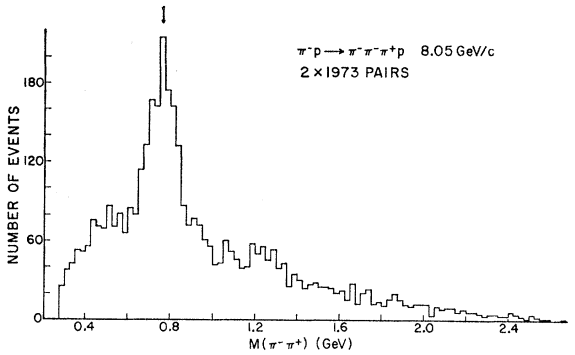

FIG. 3. Distribution of $M(\pi^-\pi^+)$. Two entries are made for each of the 1973 events. The arrow is located at 0.765 GeV.

The masses and widths of these resonances are given in Table I. These values were obtained by making maximum-likelihood fits to the mass distributions, assuming Breit-Wigner (BW) resonances combined with a background curve obtained by drawing a smooth line through the mass distribution, ignoring the resonance peaks.

The π^-p mass distribution is shown in Fig. 5. There is some indication of the neutral $N^*(1236)$. This isobar stands out more clearly when produced together with the ρ^0 meson as shown in Fig. 6. The shaded histogram is the result of making, in addition, a uniform momentum transfer cut

$$\Delta^2(\pi^-p) - \Delta^2_{\min}(\pi^-p) < 0.5(\text{GeV}/c)^2.$$

Here $\Delta^2(\pi^-p)$ is the 4-momentum transfer squared from the target proton to the outgoing π^-p system and $\Delta^2_{\min}(\pi^-p)$ is the lowest momentum transfer allowed for an event with the observed π^-p effective mass. There is some indication of the $I=\frac{1}{2}$ isobars $N^{*0}(1518)$ and $N^{*0}(1688)$.

IV. REACTION $\pi^-p \to \pi^-\rho^0p$

A. General Features of the Reaction

Work on a background model for the reaction considered in this section has been published previ-

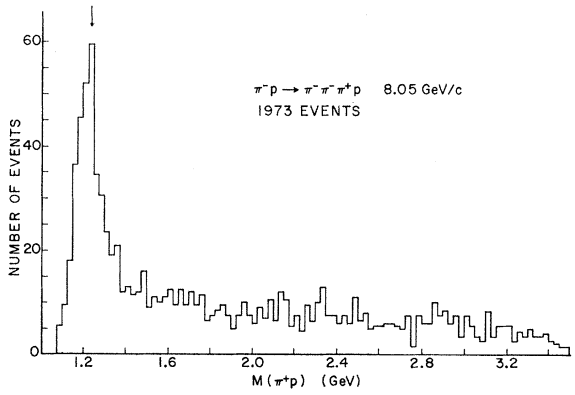

FIG. 4. Distribution of $M(\pi^+p)$. The arrow is located at 1.236 GeV.

TABLE I. Masses and widths of resonances.

	Mass (MeV)	Width (MeV)
ρ^0	766± 4	111± 8
f^0	1267±15	113±30
$N^{*++}(1236)$	1218± 4	105±10
$A_{1.5}$	1190± 4	17_{-6}^{+12}
A_2	1299±14	84_{-20}^{+30}
$A_3(\pi^- f^0)$	1610±19	100_{-30}^{+50}
$N^{*+}(1400)$	1412± 9	49_{-20}^{+30}[a]

[a] The value for the $N^*(1400)$ width is very sensitive to the choice of background. This is not included in the quoted errors.

ously.[6] It is in the reaction

$$\pi^- p \to \pi^- \rho^0 p \qquad (2)$$

that the A mesons[7] are observed as enhancements in the $\pi\rho$ system. To select events corresponding to reaction (2) we have required that at least one $\pi^-\pi^+$ combination have an effective mass in the ρ^0 region $[0.660 < M(\pi^-\pi^+) < 0.860$ GeV$]$. The scatter diagram of $\pi^-\rho^0$ effective mass versus $\pi^+ p$ effective mass shown in Fig. 7 shows that the overlap region between N^{*++} production and A production is small and exhibits no strong interference, being consistent with the sum of two overlapping bands. Since production of the $N^{*++}(1236)$ is strongly competitive with ρ^0 production, we have removed events which have a $\pi^+ p$ effective mass in the N^{*++} region $[1.125 < M(\pi^+ p) < 1.325$ GeV$]$ for our study of the $\pi\rho$ system. A further discussion of the effects of this selection is given in the description of the spin-parity analysis of the A_2.

The Dalitz plot for reaction (2) with N^{*++} events removed, shown in Fig. 8, shows a concentration of events at low $\pi^-\rho^0$ masses. In addition, it shows a smaller concentration at low $\pi^- p$ masses indicating as in Fig. 6 the formation of neutral isobars.

Figure 9 is a Chew-Low plot of $\Delta^2(p)$, the square of the 4-momentum transfer from the target proton to the outgoing proton versus the $\pi^-\rho^0$ effective mass. The scale is chosen linear in $\Delta(p)$ in order to spread the events at low $\Delta^2(p)$, where they are strongly accumulated. Most of the events are in the A region 1.0–1.4 GeV and are produced with low momentum transfer to the proton.

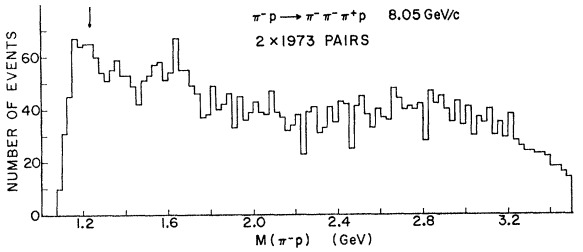

FIG. 5. Distribution of $M(\pi^- p)$. Two entries are made for each of the 1973 events. The arrow is located at 1.236 GeV.

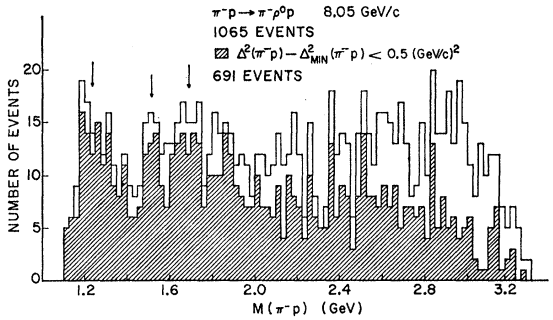

FIG. 6. Distribution of $M(\pi^- p)$ for the $\pi^-\rho^0 p$ final state. The ρ^0 cut is $0.660 < M(\pi^-\pi^+) < 0.860$ GeV. For events in which both $\pi^-\pi^+$ pairs satisfy this requirement, the pair with $M_{\pi^-\pi^+}$ closest to 0.765 GeV was chosen as the ρ^0. The shaded histogram results from making a uniform momentum-transfer cut, $\Delta^2(\pi^- p) - \Delta^2_{\min}(\pi^- p) < 0.5$ (GeV/c)^2, where $\Delta^2(\pi^- p)$ and $\Delta^2_{\min}(\pi^- p)$ are as defined in the text. The arrows are located at 1.236, 1.518, and 1.688 GeV.

Figure 10 shows the $\pi^-\rho^0$ effective-mass distribution with N^{*++} events removed and $\Delta^2(p) < 0.5$ (GeV/c)^2. There is a broad shoulder in the A_1 region, a sharp peak at 1190 MeV, hereafter called the $A_{1.5}$, and a peak corresponding to the A_2 meson. The solid curve is a maximum-likelihood fit assuming three BW resonances and a background curve combining π exchange and ρ exchange. In a previous publication[6] it was shown that the shoulder in the A_1 region is effectively reproduced by this background. The dashed curve shows the background contribution. The masses and widths of the A_2 and $A_{1.5}$ are given in Table I.

In order to investigate the significance of the $A_{1.5}$ peak, we have attempted to fit the mass distribution with A_1 and A_2 BW functions together with the background described above. Unless the assumed A_1 mass was held fixed (at 1080 MeV), its central value shifted to the $A_{1.5}$ region. Unless the A_2 width was held fixed (~90 MeV), the fitting process yielded an unreasona-

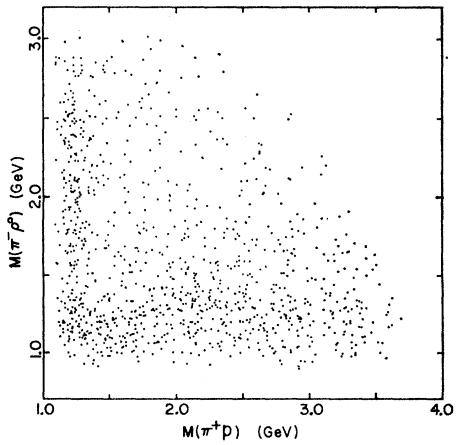

FIG. 7. Scatter diagram of $M(\pi^-\rho^0)$ versus $M(\pi^+ p)$ for the 1065 $\pi^-\rho^0 p$ events.

[6] N. M. Cason, J. W. Lamsa, N. N. Biswas, I. Derado, T. H. Groves, V. P. Kenney, J. A. Poirier, and W. D. Shephard, Phys. Rev. Letters **18**, 880 (1967).

[7] G. Goldhaber, in *Proceedings of the Thirteenth Annual International Conference on High-Energy Physics* (University of California Press, Berkeley, Calif., 1967), p. 103.

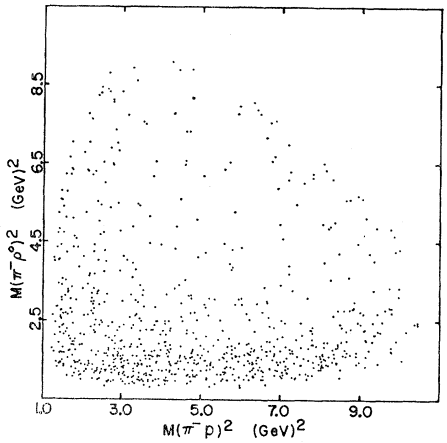

FIG. 8. Dalitz plot of $M^2(\pi^-\rho^0)$ versus $M^2(\pi^-p)$ for the 826 $\pi^-\rho^0 p$ events remaining when the $N^{*++}(1236)$ events are removed.

bly large value (~190 MeV). The fits obtained in this manner had likelihood values less than 2×10^{-3} relative to the fit, including the $A_{1.5}$. None of the fits required a significant A_1 amplitude. These facts combined with the observation of a similar effect in other experiments[7] suggest that the $A_{1.5}$ peak is not a statistical fluctuation.

We have applied the theory developed by Zemach[8] and by Frazer, Fulco, and Halpern[9] to investigate the spin and parity of the A_2. For the Dalitz plot of the three pions from the A_2 decay, the theory predicts the density of events for various assignments of the spin and parity of the A_2. The theory distinguishes between the various spin parities principally at the boundary of the Dalitz plot and in the interference region where the ρ bands overlap.

The usual way to apply the theory is to consider the $M^2(\pi^-\pi^+)$ density distribution in the ρ^0 bands of the

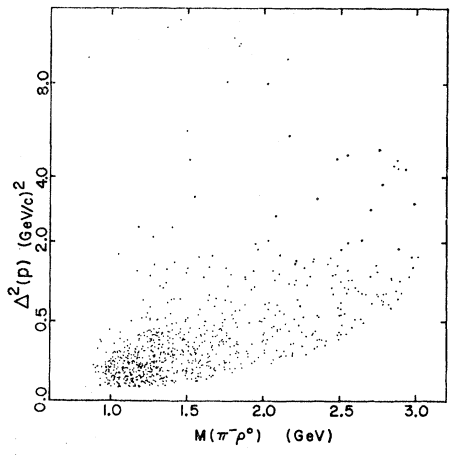

FIG. 9. Chew-Low plot of $\Delta^2(p)$ versus $M(\pi^-\rho^0)$ for the 826 $\pi^-\rho^0 p$ events remaining when the $N^{*++}(1236)$ events are removed. The scale is chosen linear in $\Delta(p)$.

[8] C. Zemach, Phys. Rev. **133**, B1201 (1964).
[9] W. R. Frazer, J. R. Fulco, and F. R. Halpern, Phys. Rev. **136**, B1207 (1964).

TABLE II. Effect of the background on the spin-parity assignment for the A_2.

% A_2	% $\pi\rho$ background	% 3π background	Likelihood ratio $2^-/2^+$	Likelihood ratio $1^+(l=0)/2^+$
60	30	10	4.9	9.4
75	15	10	97.8	191
45	45	10	0.95	1.7
100	0	0	1.8×10^{11}	2.5×10^{11}
60	0	40	0.45	1.4

Dalitz plot. Figure 11 shows the projection of this distribution for our selected A_2 events.[10] Events in the $N^{*0}(1236)$ region are shaded. We have included the $N^{*0}(1236)$ events in our A_2 sample since a study of $M^2(\pi^-p)$ versus $M^2(\pi^-\rho^0)$ for ρ^0 events shows that 80% of the events in the $N^{*0}(1236)$ A_2 overlap region are expected to be A_2 events. On the other hand, a similar study of the $N^{*++}(1236)$ A_2 overlap region indicates that only about $\frac{1}{3}$ of the overlap events are, in fact, A_2 events, and therefore none of these events has been included. A further study has shown that the results of the spin-parity analysis are not significantly affected by either of these selection criteria.

To determine theoretical distributions, Eq. (2.22) of Ref. 9 has been integrated over the ρ^0 interval chosen, and also over the A_2 mass region assuming a BW form for the A_2.[11] We have investigated the effect of background on the theoretical distributions in the following way: (1) There is a certain amount of three-pion production, not associated with the ρ^0, which enters the sample with the ρ^0 mass cut. These non-ρ^0 events are assumed to be distributed uniformly over the Dalitz plot. The Dalitz plots for events whose $\pi^-\pi^+$ mass falls just above or just below the ρ^0 are consistent with this assumption. (2) There is an additional background in the A_2 sample from $\pi\rho$ events which happen to satisfy

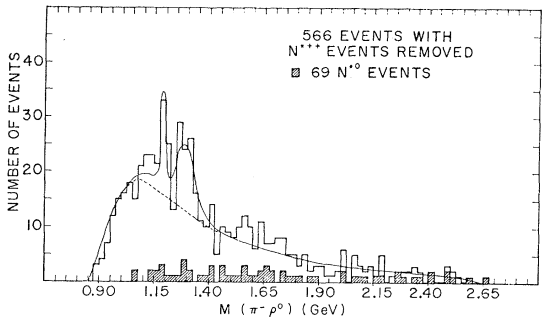

FIG. 10. Distribution of $M(\pi^-\rho^0)$ for the 566 $\pi^-\rho^0 p$ events remaining when the $N^*(1236)$ events are removed and $\Delta^2(p)$ $<0.5(\text{GeV}/c)^2$. The shaded events are consistent with the reaction $\pi^-p\to\rho^0N^{*0}(1236)$. The solid curve represents a maximum-likelihood fit to the data and the dashed curve indicates the background contribution (see text).

[10] To compare the experimental density with the theoretical curves, events in the ρ-overlap region have been entered twice on this histogram.
[11] The full width of the A_2 has been taken to be 90 MeV and that of the ρ to be 115 MeV in accordance with our data.

TABLE III. Likelihood ratios for the split A_2. We have assumed 60% A_2, 30% ρ background, and 10% 3π background.

	Likelihood ratio $2^-/2^+$	Likelihood ratio $1^+(l=0)/2^+$
A_2 (low-mass side) 1.250–1.300 GeV	3.0	8.3
A_2 (high-mass side) 1.300–1.350 GeV	73.6	54.1

the criterion $1.22 \leq M(3\pi) \leq 1.40$ GeV, but are not A_2 events, and these events will not be distributed uniformly over the Dalitz plot. The events in the two ρ bands will project as a BW peak superimposed on a phase-space background. This distribution is unfortunately very similar in form to the predicted A_2 distribution for the 2^- assignment.

The amount of 3π and $\pi\rho$ background in the sample will seriously affect the spin-parity determination. An estimate of the background may be obtained by noting that the total background under the A_2 peak in Fig. 10 is $\sim$40%; from the two-pion mass distributions of Fig. 3 we estimate that $\sim$25% of the events in the ρ^0 region are not due to ρ production. If we assume that these non-ρ events are distributed in Fig. 10 according to phase space for three out of four particles, we conclude that the 3π background amounts to $\sim$10% of the events in the A_2 peak while the $\pi\rho$ background is of the order (30 ± 15)%.

The effect of background on the fit to the theoretical curves is shown in Table II. It is evident that the likelihood ratios somewhat favor 2^- or $1^+(l=0)$ over 2^+, except where a strong background of $\pi\rho$ events is assumed present. In this case, the 2^+ assignment is about equally favored.[12] If we neglect background effects, our results would rule out the 2^+ assignment. If we assume a 40% phase space background, then the 2^+ assignment is favored over 2^-. For our best estimate of the background, namely, 60% A_2, 30% $\pi\rho$ background, and 10% 3π background the likelihood ratio $2^-/2^+$ is 4.9. For this case the χ^2 probabilities are 89% for 2^- and 47% for 2^+; the corresponding theoretical curves are shown in Fig. 11. Thus, our data favor 2^- but are also consistent with a 2^+ spin-parity assignment. We further conclude that conflicting spin-parity assignments for the A_2 recently reported[13] may be largely understood in terms of the procedures used in evaluating background.

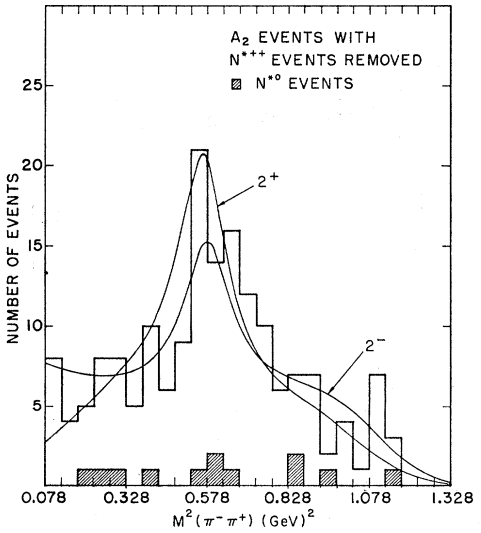

FIG. 11. Distribution of $M^2(\pi^-\pi^+)$ for the ρ^0 band of the A_2 Dalitz plot. Events in the N^{*0} region are shaded. The theoretical curves are calculated for the choice of 60% A_2, 30% $\pi\rho$ background, and 10% 3π background.

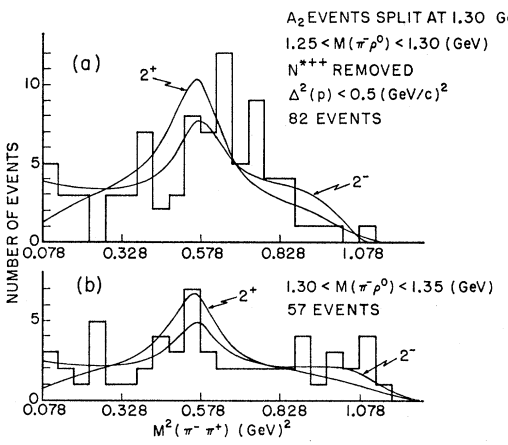

FIG. 12. Distributions of $M^2(\pi^-\pi^+)$ for the ρ^0 band of the A_2 Dalitz plot, (a) for the low-mass side of the A_2 (1.25–1.30 GeV), and (b) for the high-mass side of the A_2(1.30–1.35 GeV). The theoretical curves are calculated for the choice of 60% A_2, 30% $\pi\rho$ background, and 10% 3π background.

B. Effects of A_2 Mass Splitting on the Spin-Parity Analysis

Evidence has recently been presented for a two-peak structure in the A_2 mass region with the splitting

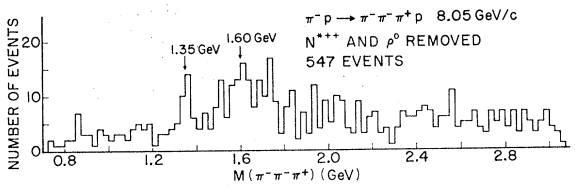

FIG. 13. Distribution of $M(\pi^-\pi^-\pi^+)$ for the 547 events remaining after $N^{*++}(1236)$ and ρ^0 events are removed.

[12] The assignments 0^-, 1^-, and $1^+(l=2)$ were also considered, but were found to be less favored than the assignments discussed here. The assignment $1^+(l=0)$ is essentially indistinguishable from the 2^- assignment for our statistics and therefore, for simplicity, we shall refer exclusively to 2^- in the discussion to follow.

[13] G. Benson, L. Lovell, E. Marquit, B. Roe, D. Sinclair, and J. Vander Velde, Phys. Rev. Letters 16, 1177 (1966); see, also, V. E. Barnes *et al.*, Ref. 1.

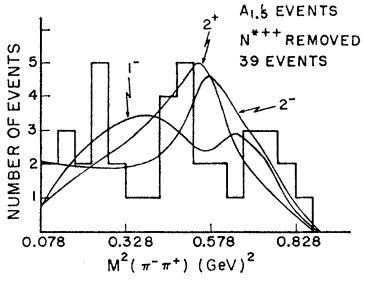

FIG. 14. Distribution of $M^2(\pi^-\pi^+)$ for the ρ^0 band of the $A_{1.5}$ Dalitz plot. The theoretical curves are for 60% A_2 and 40% $\pi\rho$ background.

occurring near 1.3 GeV.[14] Even though our statistics are not sufficient to resolve a splitting, we have reapplied our spin-parity analysis independently to the two sides of the A_2 peak. For the low-mass side we have taken $1.25 \leq M(\pi^-\rho^0) \leq 1.30$ GeV. For the high-mass side $1.30 < M(\pi^-\rho^0) \leq 1.35$ GeV was required. The values for the A_2 masses used to calculate theoretical curves were 1.275 and 1.325 GeV for the low- and high-mass sides, respectively. The width used for both was 30 MeV. We observed the same general type of dependence of the likelihood ratios on the amount and type of background used as was seen for the A_2 sample as a whole. For what we consider the best estimate of background (60% A_2, 30% $\pi\rho$ background, and 10% 3π background) likelihood ratios are presented in Table III.

The $M^2(\pi^-\pi^+)$ density distributions in the ρ^0 band of the Dalitz plot for the two sides of the A_2 peak are shown in Figs. 12(a) and 12(b). The likelihood ratios for the low-mass side are consistent with those obtained previously for the sample as a whole and are near enough to unity to make it impossible to choose between the spin parities 2^+, 2^-, or $1^+(l=0)$. For the high-mass side of the A_2 we see that 2^- and $1^+(l=0)$ are much more strongly favored than 2^+.

In Fig. 13 we show the $\pi^-\pi^-\pi^+$ mass distribution with the ρ^0 events removed. There is evidently an enhancement at 1.35 GeV. It is interesting to speculate on the possibility that the high-mass A_2 may be dominated by a direct 3π decay mode while the low-mass A_2 has mainly a $\pi\rho$ decay. Should this turn out to be the case, then the spin-parity analysis which we applied to the high-mass side of the A_2 would not be meaningful.

C. Spin-Parity Analysis of the $A_{1.5}$

With the assumption that the $A_{1.5}$ is a resonance we have attempted to determine its spin parity using the same method discussed above for the A_2 meson. The events used in the $A_{1.5}$ sample were required to have $\pi^-\rho^0$ masses between 1.175 and 1.205 GeV. In order to eliminate most of the non-ρ^0 background and to enhance the $A_{1.5}$, the ρ^0 cut was made narrower than for the A_2, $0.700 < M(\pi^-\pi^+) < 0.820$ GeV. The $M^2(\pi^-\pi^+)$ distribution in the ρ^0 band of the Dalitz plot is shown in Fig. 14 together with theoretical curves for 2^-, 2^+, and 1^- calculated assuming a 40% $\pi\rho$ background. (The curve for $1^+(l=0)$ is very similar to the curve for 2^-.) The likelihood ratios with respect to 2^+ are 19.7 for $2^-/2^+$, 17.7 for $1^-/2^+$, and 10.7 for $1^+(l=0)/2^+$.

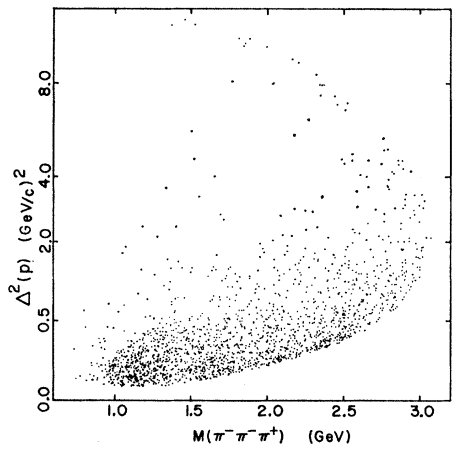

FIG. 15. Chew-Low plot of $\Delta^2(p)$ versus $M(\pi^-\pi^-\pi^+)$ for the 1973 $\pi^-\pi^-\pi^+p$ events. The scale is chosen linear in $\Delta(p)$.

[14] G. Chikovani, M. N. Focacci, W. Kienzle, C. Lechanoine, B. Levrat, B. Maglić, M. Martin, P. Schübelin, L. Dubal, M. Fischer, P. Grieder, H. A. Neal, and C. Nef, Phys. Letters **25B**, 44 (1967); D. R. O. Morrison, *ibid.* **25B**, 238 (1967).

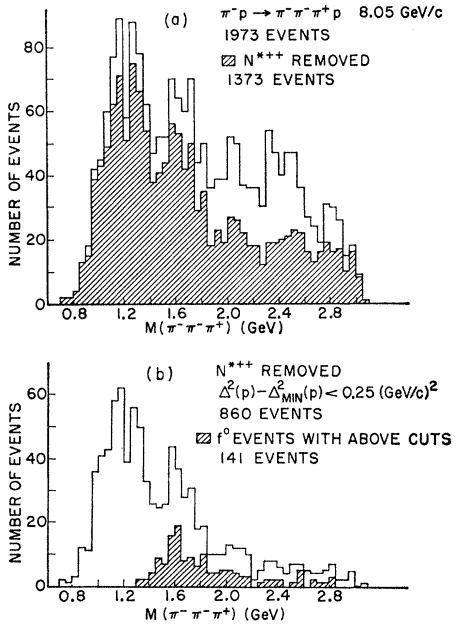

FIG. 16. Distributions of $M(\pi^-\pi^-\pi^+)$. (a) The unshaded histogram includes all 1973 events, while the shaded histogram includes only the 1373 events remaining when the $N^{*++}(1236)$ events are removed. (b) The unshaded histogram includes the 860 events remaining after an additional uniform momentum-transfer cut, $\Delta^2(p)-\Delta^2_{\min}(p) < 0.25$ (GeV/c)^2 is made; the shaded histogram includes only the 141 events in this sample with $1.150 \leq M(\pi^-\pi^+) \leq 1.350$ GeV.

We see here as we did with the A_2 analysis that the large amount of background makes a spin-parity determination very difficult.

V. A_3 ENHANCEMENT

Several groups have reported an enhancement in the 3π system near 1.64 GeV.[7,15] This peak has been called the A_3. In Fig. 15 we show the Chew-Low plot of $\Delta^2(p)$ versus $\pi^-\pi^-\pi^+$ effective mass for all events where, as before, the scale is chosen linear in $\Delta(p)$. The plot shows, in addition to the concentration in the A-meson region, 1.0–1.4 GeV, concentrations in the region around 1.6 GeV and also above 2.0 GeV. These concentrations occur at low momentum transfer to the proton.

In Fig. 16(a) we present $\pi^-\pi^-\pi^+$ mass distribution. Again we see a broad enhancement around 1.6 GeV. There is also structure[16] at 2.1, 2.4, and 2.8 GeV, all of which disappears when $N^{*++}(1236)$ events are removed as is shown in the shaded histogram. When a uniform momentum transfer cut $\Delta^2(p)-\Delta^2_{\min}(p)<0.25$ $(\mathrm{GeV}/c)^2$ is made, the distributions shown in Fig. 16(b) are obtained. The shaded distribution is the result of requiring at least one $\pi^-\pi^+$ combination to have an effective mass in the f^0 region $[1.15<M(\pi^-\pi^+)<1.35$ GeV$]$. There seems to be good evidence for an enhancement centered at 1.6 GeV with a width of about 100 MeV. It is produced at quite low momentum transfer mostly in the $\pi^- f^0$ final state. The fitted values for the mass and width of this enhancement are given in Table I. It should be noted from Fig. 10 that there is no enhancement in the $\pi^-\rho^0$ system in the 1.6-GeV region, but that the enhancement is apparent when only non-ρ^0 events are plotted as in Fig. 13.

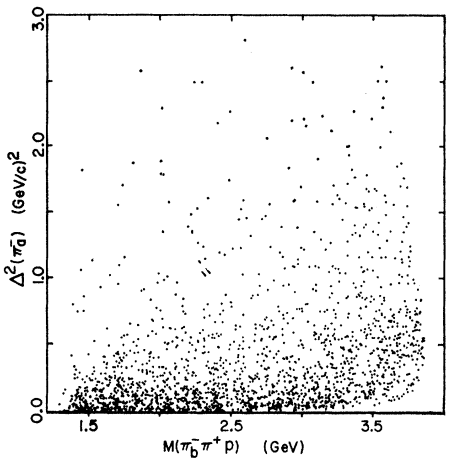

FIG. 17. Chew-Low plot of $\Delta^2(\pi_a^-)$ versus $M(\pi_b^-\pi^+p)$ for all 1973 events, where π_a^- is the negative pion with the smaller momentum transfer from the beam pion and π_b^- is the other negative pion.

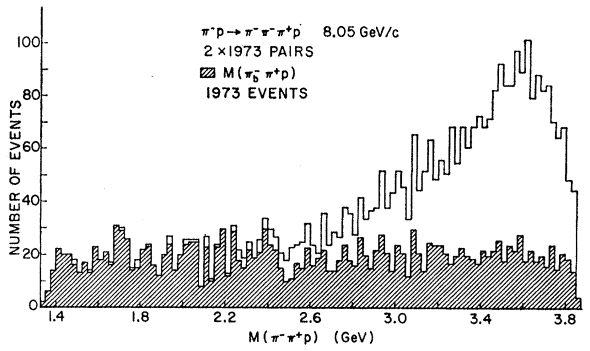

FIG. 18. Distribution of $M(\pi^-\pi^+p)$. Two entries are made for each of the 1973 events. The shaded histogram is the distribution of $M(\pi_b^-\pi^+p)$, where π_b^- is the negative pion with the larger momentum transfer from the beam pion.

The possibility that the 1.6-GeV peak may be a kinematic effect should be considered. If the ρ^0 in the diagram of the Deck mechanism[17] is replaced with an f^0 one might expect a peaking in the $\pi^- f^0$ effective mass at a value approximately equal to the A_1 mass plus the difference between the f^0 and ρ^0 masses. This value is roughly 1.6 GeV, and therefore suggests that the effect studied here may have a kinematic origin.

VI. STUDY OF AN ENHANCEMENT IN THE $\pi^-\pi^+p$ SYSTEM

A. Observation of the Enhancement

Figure 17 shows a Chew-Low plot of $\Delta^2(\pi_a^-)$ versus $\pi_b^-\pi^+p$ effective mass, where we define π_a^- as that outgoing π^- having the smaller 4-momentum transfer from the beam π^-, π_b^- as the other outgoing π^-, and $\Delta^2(\pi_a^-)$ as the 4-momentum transfer squared from beam to π_a^-. The $\pi_b^-\pi^+p$ mass distribution, shown

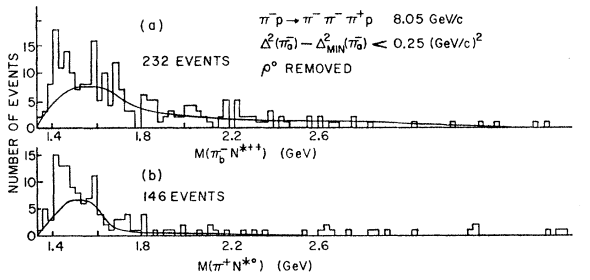

FIG. 19. Distribution of $M(\pi N^*(1236))$ with ρ^0 events removed and with a uniform momentum transfer cut, $\Delta^2(\pi_a)-\Delta^2_{\min}(\pi_a)<0.25(\mathrm{GeV}/c)^2$. (a) Distribution of $M(\pi_b^-N^{*++}(1236))$ for 232 events with $1.125\leq M(\pi^+p)\leq 1.325$ GeV; (b) distribution of $M(\pi^+N^{*0}(1236))$ for 146 events with $1.125\leq M(\pi_b^-p)\leq 1.325$ GeV. The background curves shown in (a) and (b) are discussed in the text.

[15] I. A. Vetlitsky, V. M. Guszavin, G. K. Kliger, V. Z. Kolganov, A. V. Lebedev, G. S. Lomkazi, V. T. Smoljankin, A. P. Sokolov, and E. A. Sisoew, Phys. Letters **21**, 579 (1966); F. Conte, G. Tomasini, D. Cords, P. Dittmann, P. v. Handel, B. Hellwig, L. Mandelli, S. Ratti, V. Russo, A. Silvestri, G. Vegni, P. Daronian, A. Daudin, B. Gandois, C. Kochowski, C. Lewin, and L. Mosca (unpublished).

[16] Whether this structure is a kinematic reflection of $N^{*++}(1236)$ production or is of an interference nature is not clear. Our experiment does not allow an analysis of the peaks associated with $N^{*++}(1236)$ production because of insufficient statistics.

[17] R. J. Deck, Phys. Rev. Letters **12**, 340 (1964).

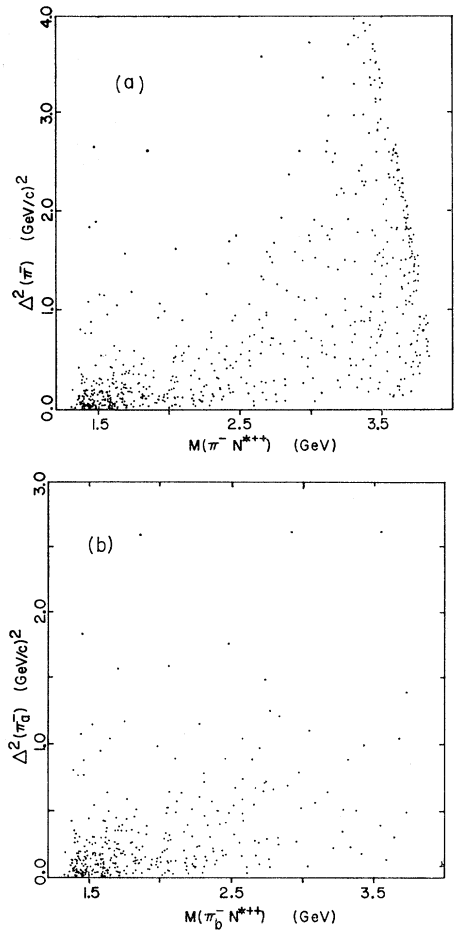

FIG. 20. Chew-Low plots of (a) $\Delta^2(\pi^-)$ versus $M(\pi^- N^{*++}(1236))$ with two points per event, and (b) $\Delta^2(\pi_a^-)$ versus $M(\pi_b^- N^{*++}(1236))$. These plots are for the 361 $N^{*++}(1236)$ events remaining after ρ^0 events are removed. In (a) 72 points are outside the plot.

shaded in Fig. 18, is very flat, giving no evidence for isobar formation. However, when the $\pi^+ p$ or $\pi_b^- p$ effective mass is required to be in the $N^*(1236)$ band, we observe a mass peaking in the $\pi_b^- \pi^+ p$ system between 1.4 and 1.5 GeV. This is shown in the $\pi N^*(1236)$ mass distributions in Figs. 19(a) and 19(b). In this figure and in the following analysis we have removed events containing a ρ^0 in order to obtain a cleaner sample of $N^*(1236)$ events and have made a uniform momentum transfer cut $\Delta^2(\pi_a^-) - \Delta^2_{\min}(\pi_a^-) < 0.25$ (GeV/c)^2.

To study this enhancement further, we consider the Chew-Low plots, $\Delta^2(\pi^-)$ versus $\pi^- N^{*++}(1236)$ effective mass in Fig. 20(a) (with two entries per event), and $\Delta^2(\pi_a^-)$ versus $\pi_b^- N^{*++}(1236)$ effective mass in Fig. 20(b). From this figure we can see that the events in the concentration between 1.4 and 1.5 GeV are produced very peripherally.

B. Is the Enhancement a Kinematic Effect?

We have calculated a background curve for the $\pi^- N^{*++}(1236)$ mass distribution, assuming the dominance of one-pion exchange (Fig. 21) for the reaction

$$\pi^- p \to \pi^- \pi^- N^{*++}(1236). \quad (3)$$

Fake events were generated by a Monte Carlo technique. The Monte Carlo events were required to have an exponential momentum transfer distribution from the target proton to the $N^{*++}(1236)$ which reproduced the experimental momentum transfer distribution. The form used was $\exp[-7.5\Delta^2(p, N^{*++}(1236))]$. The decay angular distribution of the $N^{*++}(1236)$ was required to be of the form $(1+3\cos^2\theta_{pp})$. The $\pi^-\pi^-$ effective-mass distribution for the Monte Carlo events was required to reproduce the experimental distribution. For $\pi^-\pi^-$ effective masses above 1 GeV we required that the distribution of the scattering angle between the incident beam and one of the outgoing pions in the $\pi^-\pi^-$ rest system have an exponential $\Delta^2(\pi^-, \pi^-)$ dependence.[18] Angular distributions for πp, Kp, and pp elastic scattering are very similar at high energies, all behaving approximately as $\exp(-8\Delta^2)$,[19] and we have used the same exponential dependence for the $\pi^-\pi^-$ elastic scattering. For $\pi^-\pi^-$ effective masses below 1 GeV the scattering angle was required to have an isotropic distribution.[20]

The same cuts were applied to the Monte Carlo events as were applied to the real events. Background curves for the $\pi_b^- N^{*++}(1236)$ and $\pi^+ N^{*0}(1236)$ effective-mass distributions obtained in this way are shown as the solid lines in Figs. 19(a) and 19(b). The curve in Fig. 19(a) is normalized to the data for $M(\pi_b^- N^{*++}(1236)) > 1.5$ GeV. [We use the fact that some of the Monte Carlo $\pi^-\pi^- N^{*++}(1236)$ events have a $\pi^- p$ effective-mass combination in the $N^{*0}(1236)$ mass band to obtain the curve shown in Fig. 19(b).] It is clear from these curves that the kinematic interpretation of the $\pi^-\pi^+ p$ enhancement does not fit the data.[21]

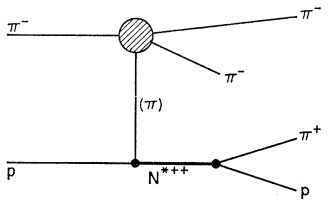

FIG. 21. One-pion-exchange diagram for the reaction $\pi^- p \to \pi^- \pi^- N^{*++}(1236)$.

[18] A $\pi^-\pi^-$ effective mass of 1 GeV would correspond to a laboratory momentum of about 3.5 GeV/c for a pion incident on a target pion at rest. We therefore feel that for $\pi^-\pi^-$ masses above 1 GeV we are in the diffraction region.

[19] For a list of references see N. N. Biswas, N. M. Cason, I. Derado, V. P. Kenney, J. A. Poirier, and W. D. Shephard, Phys. Rev. Letters **18**, 273 (1967).

[20] J. Alitti, J. P. Baton, A. Berthelot, B. Deler, W. J. Fickinger, and N. Neveu-René, Nuovo Cimento **35**, 1 (1965); G. Wolf, Phys. Letters **19**, 328 (1965). From these references, it is clear that s wave dominates the π-π $T=2$ scattering below energies of 0.8 GeV.

[21] Variations up to $\exp[-20\Delta^2(\pi^-, \pi^-)]$ and $\exp[-20\Delta^2(p, N^{*++}(1236))]$ in the peripherality assumed in the Monte Carlo calculation do not improve the agreement significantly.

C. Resonance Interpretation of the Enhancement

Since the enhancement does not seem to be caused by a simple kinematic effect, we now consider the possibility of its being a resonance. In particular, a very likely possibility is that we are observing the "Roper resonance."[22] We shall refer to this resonance as the $N^*(1400)$. We believe that we may be observing the $N^*(1400)$ for several reasons. First, the mass obtained from a maximum-likelihood fit using the background curve shown in Fig. 19(a) is consistent with earlier determinations.[22,23] (See Table I.) Second, the fact that the phase-shift analysis[22] predicts a high inelasticity for the $N^*(1400)$ is consistent with our observation of the enhancement in the $\pi^-\pi^+p$ state. Finally, since the $N^*(1400)$ has the same quantum numbers as the nucleon, its production via diffraction dissociation[24] is possible, and the highly peripheral nature of the production of our observed enhancement is consistent with such an interpretation.

Although our analysis appears to establish the existence of a $\pi N^*(1236)$ decay mode of the $N^*(1400)$, this is not necessarily so since the very low Q value for $N^*(1400) \to \pi^-\pi^+p$ requires that the πN effective mass fall into the $N^*(1236)$ region. It has, in fact, been suggested[25] that the primary decay mode of the $N^*(1400)$ should be σp (where σ is a low mass $\pi^+\pi^-$ s-wave effect).

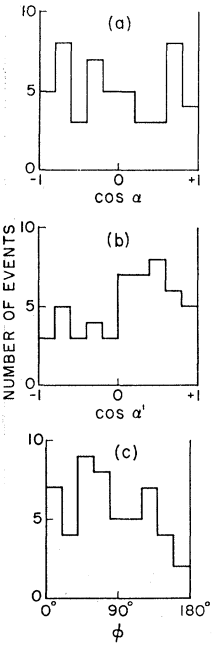

FIG. 23. (a) Distribution of cosα, where α is the angle between the target proton and π_b^- in the $N^*(1400)$ rest frame. The distribution includes 51 events with $1.125 \leq M(\pi^+p) \leq 1.325$ GeV; with $\Delta^2(\pi_a^-) - \Delta^2_{\min}(\pi_a^-) < 0.25$ (GeV/c)^2; with $1.375 \leq M(\pi_b^-\pi^+p) \leq 1.475$ GeV; and with $M(\pi^-\pi^+) \leq 0.660$ GeV or $M(\pi^-\pi^+) \geq 0.860$ GeV. (b) Distribution of cosα', where α' is the angle between the outgoing proton in the $N^*(1236)$ rest system and the target proton in the $N^*(1400)$ rest system for the same events. (c) Distribution of ϕ, the angle between the plane formed by the incident beam and π_a^- and the plane formed by the $N^{*++}(1236)$ and π_b^- in the laboratory system for the same events.

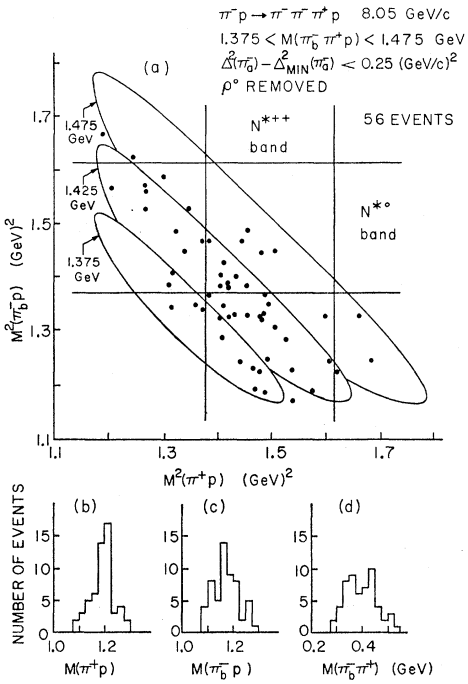

FIG. 22. (a) Dalitz plot of $M^2(\pi_b^-p)$ versus $M^2(\pi^+p)$ for the 56 events with $1.375 < M(\pi_b^-\pi^+p) < 1.475$ GeV, with $\Delta^2(\pi_a^-) - \Delta^2_{\min}(\pi_a^-) < 0.25$ (GeV/c)^2, and with ρ^0 events removed. Kinematic limits are shown for $M(\pi_b^-\pi^+p)$ values of 1.375, 1.425, and 1.475 GeV. The corresponding two-particle mass distributions are (b) $M(\pi^+p)$, (c) $M(\pi_b^-p)$, and (d) $M(\pi_b^-\pi^+)$.

Figure 22(a) shows the Dalitz plot of $M^2(\pi^-p)$ versus $M^2(\pi^+p)$ for events with $1.375 < M(\pi_b^-\pi^+p) < 1.475$ GeV, with $\Delta^2(\pi_a^-) - \Delta^2_{\min}(\pi_a^-) < 0.25$(GeV/$c$)^2 and ρ^0 events removed. The corresponding two-particle mass distributions are shown in Figs. 22(b)–22(d). It appears that the peaking in the π^+p mass distribution is more prominent than in the other mass distributions and suggests that $N^*(1400) \to \pi N^*(1236)$ is preferred over $N^*(1400) \to \sigma p$. If this is the case, we should observe, for an $I = \frac{1}{2}$ resonance, the branching ratio

$$\frac{N^*(1400) \to \pi^- N^{*++}(1236)}{N^*(1400) \to \pi^+ N^{*0}(1236) \to \pi^+\pi^- p} = 9,$$

and hence, we do not expect to detect the $N^{*0}(1236)$ peak in the π^-p distribution. This appears to be consistent with the data.

If the $N^*(1400)$ has $J^P = \frac{1}{2}^+$ and is produced via diffraction dissociation, we expect its decay angular distribution as well as that of the $N^*(1236)$ coming from $N^*(1400)$ decay to be isotropic. Figure 23(a) shows the distribution of cosα, where α is the angle between the target proton and π_b^- in the $N^*(1400)$ rest frame. The distribution is consistent with isotropy (χ^2 probability of 60%). Figure 23(b) shows the distribution of cosα', where α' is the angle between the outgoing proton in the $N^*(1236)$ system and the target proton in the $N^*(1400)$ system. Although there

[22] L. D. Roper, Phys. Rev. Letters **12**, 340 (1964).
[23] K. J. Foley, R. S. Jones, S. J. Lindenbaum, W. A. Love, S. Ozaki, E. D. Platner, C. A. Quarles, and E. H. Willen, Phys. Rev. Letters **19**, 397 (1967).
[24] M. L. Good and W. D. Walker, Phys. Rev. **120**, 1857 (1960); M. Ross and L. Stodolsky, *ibid.* **149**, 1172 (1966); L. Stodolsky, Phys. Rev. Letters **18**, 973 (1967).
[25] For references see C. Lovelace, CERN Report No. 66/1257/5-Th. 705, 1966 (unpublished).

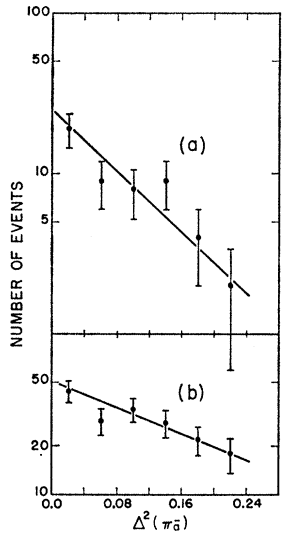

FIG. 24. Distribution of $\Delta^2(\pi_a^-)$ for events with $1.125 \leq M(\pi^+p) \leq 1.325$ GeV; with $\Delta^2(\pi_a^-) - \Delta^2_{\min}(\pi_a^-) < 0.25$ (GeV/c)^2; and with $M(\pi^-\pi^+) \leq 0.660$ GeV or $M(\pi^-\pi^+) \geq 0.860$ GeV. (a) The distribution for the 51 events with $1.375 \leq M(\pi_b^-\pi^+p) \leq 1.475$ GeV [i.e., $N^*(1400)$ events]. The line is $\exp[-11\Delta^2(\pi_a^-)]$. (b) The distribution for the 175 events with $M(\pi_b^-\pi^+p) < 1.375$ GeV or $M(\pi_b^-\pi^+p) > 1.475$ GeV [i.e., non-$N^*(1400)$ events].

is some fore-aft asymmetry, the distribution is also consistent with isotropy (χ^2 probability of 65%). Finally, Fig. 23(c) shows the distribution in ϕ, the Treiman-Yang angle, defined as the angle between the plane formed by the incident beam and π_a^- and the plane formed by the $N^{*++}(1236)$ and π_b^- in the laboratory system. It is also consistent with isotropy (χ^2 probability of 19%) as expected for a "diffractionlike" process.

We have compared our data with a specific model[26] which assumes that the reaction $\pi^-p \to \pi^-N^*(1400)$ proceeds via coherent regeneration due to diffraction dissociation of the proton. This model relates the process $\pi^-p \to \pi^-N^*(1400)$ to π^-p and pp elastic scattering, and predicts that the $N^*(1400)$ is produced with the cross section[27]

$$d\sigma/d\Delta^2 = 2.8 \exp[-11\Delta^2(\pi_a^-)].$$

Figure 24(a) shows the $\Delta^2(\pi_a^-)$ distribution for events in the $N^*(1400)$ region. The curve shown is

$$\exp[-11\Delta^2(\pi_a^-)]$$

and is normalized to the data. The curve fits quite well with a χ^2 probability of 63%. Figure 24(b) shows the $\Delta^2(\pi_a^-)$ distribution for events outside the $N^*(1400)$ region. Here the distribution is much flatter than for the $N^*(1400)$ region. The curve, shown for reference, is $\exp[-4.6\Delta^2(\pi_a^-)]$.

The dissociation model predicts a cross section of 0.24 mb for the reaction $\pi^-p \to \pi^-N^*(1400)$ with $\Delta^2(\pi_a^-) < 0.25$ GeV^2. To compare this with our data, we must take into account other decay modes of the $N^*(1400)$ as well as unseen charge states of the $\pi N^*(1236)$ decay mode. Since the $N^*(1400)$ is believed to decay into πN about 70% of the time,[28] we assume that the $\pi N^*(1236)$ decay occurs 30% of the time. Furthermore, we have studied only the $\pi^-N^{*++}(1236)$ decays, which comprise 50% of the $\pi N^*(1236)$ decay mode. Thus the model would predict a cross section of $0.24(0.3)(0.5) = 0.036$ mb for production of $N^*(1400)$ with decay into $\pi^-N^{*++}(1236)$. Our observed cross section is 0.019 ± 0.006 mb, in fair agreement with this model.[29]

[26] P. K. Williams, University of Michigan (private communication).

[27] A smaller cross section with a steeper Δ^2 dependence is expected if pion dissociation is significant.

TABLE IV. Cross sections.[a]

	Cross section (mb)	Percent
$\pi^-p \to \pi^-\pi^-\pi^+p$	1.27 ±0.07	
$\pi^-p \to \pi^-\rho^0p$	0.56 ±0.04	44.4±3.0
$\to A_{1.5}p$	0.015±0.005	
$\to A_2p$	0.042±0.012	
$\to \rho^0N^{*0}(1236)$	0.028±0.007	
$\pi^-p \to \pi^-f^0p$	0.088±0.018	7.0±1.4
$\to A_3(\pi^-f^0)p$	0.021±0.008	
$\pi^-p \to \pi^-\pi^-N^{*++}(1236)$	0.32 ±0.05	25.1±4.0
$\to \pi^-N^{*+}(1400)$	0.019±0.006	
$\pi^-p \to \pi^-\pi^-\pi^+p$ (nonresonant)	0.30 ±0.07	23.5±5.2

[a] These cross sections are not corrected for unseen decay modes.

VII. CROSS SECTIONS

The total cross section for the reaction $\pi^-p \to \pi^-\pi^-\pi^+p$ has been determined by considering the density of the expanded hydrogen, the pion path length corrected for beam contamination, and the number of events in the fiducial volume (corrected for scanning, flare loss, event-selection criteria, and unmeasurable events).[30] Cross sections for resonance production have been obtained from the maximum-likelihood fits to the data which yielded the masses and widths in Table I. The results are given in Table IV.

ACKNOWLEDGMENTS

We wish to thank Brookhaven National Laboratory and its staff members for their cooperation and assistance in performing this experiment. Professor M. Ross suggested the search for the $N^*(1400)$ in the $\pi^-\pi^+p$ system. We are grateful for the assistance of John B. Annable and Robert J. Schlentz. The cooperation of the Notre Dame Computing Center is appreciated. Finally, we would like to thank our scanning staff for its excellent work.

[28] P. Bareyre, C. Bricman, A. V. Stirling, and G. Villet, Phys. Letters 18, 342 (1965).

[29] It is interesting to note that the results quoted in Ref. 23 for production of the $N^*(1400)$ in π^-p interactions are also consistent with the dissociation model. Their fitted expression for $d\sigma/d\Delta^2$ is $2.5 \exp(-12.1\Delta^2)$.

[30] J. A. Poirier, N. N. Biswas, N. M. Cason, I. Derado, V. P. Kenney, W. D. Shephard, E. H. Synn, H. Yuta, W. Selove, R. Ehrlich, and A. L. Baker, Phys. Rev. 163, 1462 (1967).